Energy Conversion and Management 50 (2009) 1401–1410

Contents lists available at ScienceDirect

Energy Conversion and Management

journal homepage: www.elsevier.com/locate/enconman

Robust control of an industrial boiler system; a comparison between two approaches: Sliding mode control & H_∞ technique

Hamed Moradi *, Firooz Bakhtiari-Nejad, Majid Saffar-Avval

Energy and Control Centre of Excellence, Department of Mechanical Engineering, Amirkabir University of Technology, Tehran, Iran

ARTICLE INFO

Article history:
Received 28 July 2008
Accepted 8 March 2009
Available online 5 April 2009

Keywords:
Boiler system
Model uncertainties
Sliding mode control
H_∞ Technique
μ-Synthesis

ABSTRACT

To achieve a good performance of the utility boiler, dynamic variables such as drum pressure, steam temperature and water level of drum must be controlled. In this paper, a linear time invariant (LTI) model of a boiler system is considered in which the input variables are feed-water and fuel mass rates. However this dynamic model may associate with uncertainties. With considering the uncertainties of the dynamic model, a sliding mode controller is designed. After representation of the uncertain dynamic system in general control configuration and modelling the parametric uncertainties, nominal performance, robust stability and robust performance are analyzed by the concept of structured singular value μ. Using an algorithm for μ-analysis and applying an inversed-base controller, robust stability and nominal performance are guaranteed but robust performance is not satisfied. Finally, an optimal robust controller is designed based on μ-synthesis with DK-iteration algorithm. Both optimal robust and sliding mode controllers guarantee robust performance of the system against the uncertainties and result in desired time responses of the output variables. By applying H_∞ robust control, system tracks the desire reference inputs in a less time and with smoother time responses. However, less control efforts, feedwater and fuel mass rates, are needed when the sliding mode controller is applied.

1. Introduction

Boiler unit, that produces steam, is one of the critical components of the power plant. This is because the steam flow rate, its temperature and pressure affect the performance of power plant. Although the steam production is varied during plant operation, output variables such as steam pressure, temperature and water level of drum must be maintained at their respected values. Therefore, regulation of water level of drum and tracking the load variation commands of drum pressure and power output are expected from a boiler–turbine system. However, the physical constraints exerted on the actuators must be satisfied by the control signals. These constraints can be the magnitude and saturation rate for the control valves of the fuel, steam and feed-water flow [1,2]. Two configurations exist to generate electricity. First, a boiler–turbine unit in which the steam is produced by a single boiler and is fed to single turbine. In the second one, several boilers generate steam which is conducted to collector and then distributed to several turbines. Industrial plants usually use this type of configuration. As the boiler–turbine has a quick response to the electricity demands from a power grid, it is preferred to have collector type systems [3].

A boiler–turbine unit is a nonlinear complex system. Several dynamic models of the boiler system have been developed [4–6] and there are several simulation packages such as SYNSIM for steam plants [7]. Various control methods have been applied to boiler or boiler–turbine controller design, e.g., gain scheduling and feedback linearization [1,2], adaptive control [8], Linear Quadratic Gaussian (LQG) [9], predictive control [10] and intelligent control [11–13]. Also some aspects related to robust control and mixed sensitivity [14–16] have been applied in different ways. But in these works, the parametric uncertainties associated with multivariable dynamic model are not considered. In addition, to achieve a good performance of boiler unit, the application of μ-synthesis based on DK-iteration have not been used in previous studies. A control system is robust if it is insensitive to differences between the actual system and the model of the system which was used to design the controller. These differences are referred to as model uncertainty. The H_∞ robust control technique is used to check if the design specifications are satisfied even for the worst-case uncertainty. In this approach, a mathematical representation of the model uncertainty is found. Then it is determined if the stability and performance specifications are satisfied for all plants in the uncertainty set (robust stability and robust performance) [17].

In this paper, a linear time invariant (LTI) model of the boiler system is considered. The input variables are feedwater mass rate and fuel mass rate while the output variables are water level of drum, drum pressure and steam temperature. After modelling

* Corresponding author. Tel.: +98 2164543417; fax: +98 66419736.
E-mail addresses: hamed.moradi1@gmail.com (H. Moradi), baktiari@aut.ac.ir (F. Bakhtiari-Nejad).

0196-8904/$ - see front matter © 2009 Elsevier Ltd. All rights reserved.
doi:10.1016/j.enconman.2009.03.002

the parametric uncertainties, a sliding mode controller is designed. Then the uncertain system is represented in the form of general control configuration and unstructured uncertainty is considered in the form of multiplicative input uncertainty. On the other hand, to achieve the goals of disturbance rejection and command tracking, the sensitivity function must have a special shape which is obtained by considering a suitable performance weight function. Using an algorithm for μ-analysis and applying an inversed-base controller, robust stability and nominal performance are achieved for perturbed plants. Finally, using μ-synthesis with DK-iteration algorithm, an optimal robust controller is designed. Both optimal robust controller and sliding mode controller guarantee the robust performance of the uncertain system.

2. Linear time invariant model of boiler

2.1. Boiler performance

A watertube boiler is considered in which the water flows in the tubes and fire is supplied around it. The performance of this boiler is shown in Fig. 1 [18,19]. The input variables u_1, u_2 and u_3 are feedwater mass rate, fuel mass rate and spray attemperator mass rate (kg/s) and output variables y_1, y_2 and y_3 are water level of drum (m), drum pressure (Mpa) and steam temperature (°C), respectively.

To control the output variables, the real model of utility boiler system presented by Tan and Marquez [18] is used. To distribute the steam, this plant utilizes a complex collector system, which includes collectors at four different pressure levels (6.306 – 4.24 – 1.068 – 0.372 Mpa). As shown in Fig. 2, 6.036 Mpa collector receives steam from three utility-type (UB) boilers burning refinery gas, three CO-type boilers burning cocker off gas and refinery gas, and two once-through steam generators (OTSG's). Then the steam is distributed through the collector system to the several steam turbines to generate electricity.

For proper performance of the boiler system, although, the amount of steam demanded by users is varied but the steam pressure of the 6.306 Mpa collector must be maintained constant. Also, to prevent over-heating of drum components or flooding of steam lines the amount of water in the steam drum must be kept constant. On the other hand, the steam temperature must be maintained at the desired level to prevent over-heating of the superheaters and to prevent wet steam entering turbines.

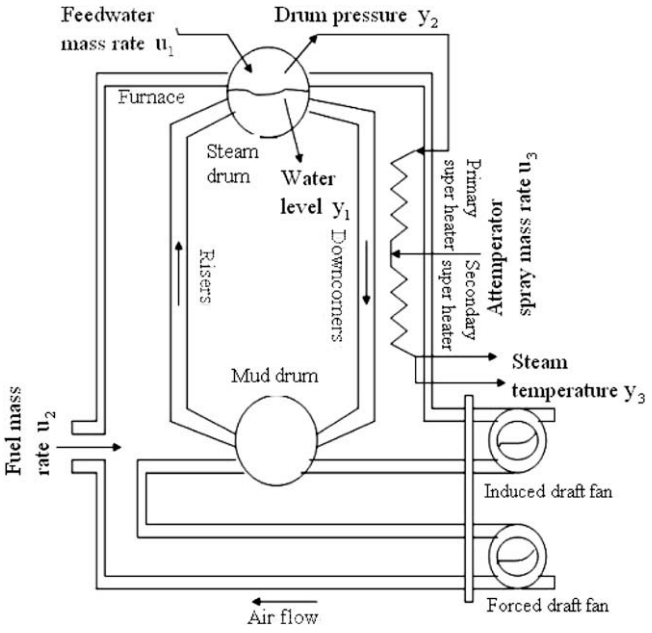

Fig. 1. Schematic of boiler performance [18].

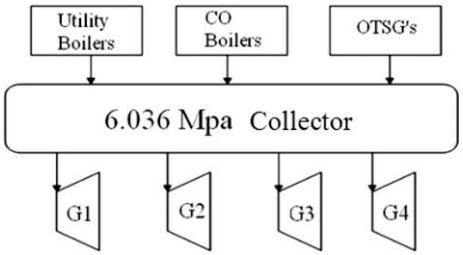

Fig. 2. Simple schematic of Syncrude plant model [18].

2.2. Dynamic model of the boiler system

For the operating point mentioned in the previous section, collecting input–output data on SYNSIM and using the MATLAB Systems Identification Toolbox, the LTI model for the boiler system is obtained as follows [7,18]:

$$\begin{bmatrix} y_1 \\ y_2 \\ y_3 \end{bmatrix} = \begin{bmatrix} \frac{(-0.16s^2+0.052s+0.0014)\times 10^{-3}}{s^2+0.0268s+0.000168} & \frac{(3.1s-0.032)\times 10^{-3}}{s^2+0.0415s+0.00043} & 0 \\ \frac{-0.0395\times 10^{-3}}{s+0.018} & \frac{2.51\times 10^{-3}}{s+0.0157} & \frac{(0.588s^2+0.2015s+0.0009)\times 10^{-3}}{s^2+0.0352s+0.000142} \\ \frac{-0.000118s+0.000139}{s^2+0.01852s+0.000091} & \frac{0.448s+0.0011}{s^2+0.0127s+0.000095} & \frac{0.582s-0.0243}{s^2+0.1076s+0.00104} \end{bmatrix} \times \begin{bmatrix} u_1 \\ u_2 \\ u_3 \end{bmatrix} \quad (1)$$

After testing several alternative model structures, it was found that a third-order model can fit the input–output data fairly well. After finding the zeros and dominant poles of the transfer functions of Eq. (1) and according to the results of [2,18–20], water level of drum y_1 mainly is affected by feedwater mass rate u_1. Similarly, the drum pressure y_2 and the steam temperature y_3 mainly are affected by the fuel mass rate u_2 (Appendix A). Also, it can be shown that the effect of spray attemperator mass rate u_3 on output variables is negligible [18]. So, the transfer function between y_1 and u_1 is approximated as follows such that, at least, the time response of the approximated model to step and ramp inputs are the same as real model:

Case-1:

$$G_1(s) = \frac{Y_1(s)}{U_1(s)} = \frac{k_a}{s^3 + a_1 s^2 + a_2 s + a_3} \quad (2a)$$

Using a similar procedure, other transfer functions will be [19]:

Case-2:

$$G_2(s) = \frac{Y_2(s)}{U_2(s)} = \frac{k_b}{s^3 + b_1 s^2 + b_2 s + b_3} \quad (2b)$$

Case-3:

$$G_3(s) = \frac{Y_3(s)}{U_2(s)} = \frac{k_c}{s^3 + c_1 s^2 + c_2 s + c_3} \quad (2c)$$

where the constants are given in Table 1.

Table 1
Average values of constants in G_1, G_2, G_3.

$\bar{a}_1$	4.7×10^{-2}	$\bar{b}_1$	4.5×10^{-2}	$\bar{c}_1$	1.23×10^{-1}
$\bar{a}_2$	7×10^{-4}	$\bar{b}_2$	6.5×10^{-4}	$\bar{c}_2$	1.7×10^{-3}
$\bar{a}_3$	3.4×10^{-6}	$\bar{b}_3$	3×10^{-6}	$\bar{c}_3$	1.6×10^{-6}
$\bar{k}_a$	1.2×10^{-4}	$\bar{k}_b$	2.5×10^{-5}	$\bar{k}_c$	3.3×10^{-3}

3. Sliding mode control

A simple approach to robust control is the sliding mode methodology in which the nth-order problem is replaced by an equivalent first-order system. Consider the nonlinear dynamic system with a single-input [21]:

$$y^{(n)} = f(\bar{y}) + g(\bar{y})u \tag{3}$$

where the scalar y is the output, u is the control input and $\bar{y} = [y\ \dot{y} \dots y^{(n-1)}]$ is the state vector. $f(\bar{y})$ and $g(\bar{y})$ are nonlinear functions of time and states. These functions may have uncertainties, but they are bounded by known continuous functions of y and t. A sliding surface can be defined as

$$s(y;t) = \left(\frac{d}{dt} + \lambda\right)^{n-1} \tilde{y}$$

where $\tilde{y} = y - y_d$ is the tracking error, y_d is the desired state to be tracked and λ is a positive constant. The control law u of Eq. (3) must be chosen such that:

$$\frac{1}{2}\frac{d}{dt}s^2 = s\dot{s} \leqslant -\eta|s| \tag{4}$$

where η is a positive constant. Eq. (4) indicates that the squared distance to the surface decreases along all system trajectories, so it causes the trajectories move towards the surface s. Since three transfer functions in Eq. (2) are represented by a third-order differential equation, consider

$$y^{(3)} = f(y, \dot{y}, \ddot{y}) + bu$$

where the nonlinear dynamic function $f(y, \dot{y}, \ddot{y})$ is not exactly known, but estimated as $\hat{f}(y, \dot{y}, \ddot{y})$ and control gain b is varied between two extreme limits as $0 < b_{\min} < b < b_{\max}$. The estimation error on f is assumed to be bounded by some known function $F(y, \dot{y}, \ddot{y})$ such that:

$$|\hat{f} - f| \leqslant F \tag{5}$$

In order $y(t)$ to track $y_d(t)$, sliding surface $s = 0$ is defined as

$$s = \left(\frac{d}{dt} + \lambda\right)^{(2)} \tilde{y} = \dddot{\tilde{y}} + 2\lambda\ddot{\tilde{y}} + \lambda^2\dot{\tilde{y}}$$

where $\tilde{y} = y - y_d$ is the tracking error. The best approximation $\hat{u}$ of a continuous control law that would achieve $\dot{s} = 0$ is

$$\hat{u} = -\hat{f} + y_d^{(3)} - 2\lambda\ddot{\tilde{y}} - \lambda^2\dot{\tilde{y}} \tag{6}$$

In spite of the uncertainty associated with the dynamics f, to satisfy the sliding condition, a discontinuous term across the surface $s = 0$ is added as follows:

$$u = \hat{b}^{-1}[\hat{u} - K \cdot \mathrm{sgn}(s)]; \quad \hat{b} = (b_{\min} b_{\max})^{1/2}$$

where sgn is the sign function. It can be shown that by letting

$$K \geqslant \beta(F + \eta) + (\beta - 1)|\hat{u}|; \quad \beta = (b_{\max}/b_{\min})^{1/2} \tag{7}$$

Condition in Eq. (4) will be satisfied [21]. To improve performance, chattering must be eliminated. To achieve this, the control discontinuity must be smoothed in a thin boundary layer around the switching surface. So, the sign function is replaced by the saturation function, and the control input u is modified to

$$u = \hat{b}^{-1}[\hat{u} - K \cdot sat(s/\Phi)]$$
$$sat(s/\Phi) = \begin{cases} s/\phi & |s| \leqslant \Phi \\ \mathrm{sgn}(s) & \text{otherwise} \end{cases} \tag{8}$$

where Φ is the thickness of boundary layer and $\varepsilon = \Phi/\lambda^{n-1}$ is the width of boundary layer. Using control law of Eq. (8) guarantees the tracking within a precision ε.

4. Robust control of the boiler system

The general control configuration is shown in Fig. 3a where P is the generalized plant and K is the generalized controller [22]. The overall objective is to minimize some norm of the transfer function from w to z. Therefore, based on the information in v, the controller design problem is to find a controller K which produces the control signal u that counteracts the influence of w on z by minimizing the closed loop norm $\|T_{wz}\|_\infty$.

The matrix Δ is a block diagonal matrix that includes all possible perturbations to the system. It is usually normalized such that $\|\Delta\|_\infty \leqslant 1$. The block diagram of Fig. 3a is in terms of P which is used for synthesis. By using K to close a lower loop around P, this block diagram can be transformed into the block diagram in terms of N for analysis as shown in Fig. 3b. By partitioning P according to the controller K and using lower linear fractional transformation (LFT) results in (Appendix B)

$$N = F_L(P, K) = P_{11} + P_{12}K(I - P_{22}K)^{-1}P_{21}$$

As shown in Fig. 3b, Δ is used to close the upper loop around N. Therefore the perturbed (uncertain) transfer function from external inputs w to external outputs z can be evaluated by an upper linear fractional transformation (LFT) as

$$z = F_u(N, \Delta)w; \quad F_u(N, \Delta) = N_{22} + N_{21}\Delta(I - N_{11}\Delta)^{-1}N_{12} \tag{9}$$

Suitable practical approaches such as DK-iteration can be used to find the μ-optimal controller. In a practical case, each source of uncertainty is represented by a perturbation block Δ_i which is normalized such that $\|\Delta_i\| \leqslant 1$.

4.1. H_∞ Control design

Consider a schematic of H_∞ design as shown in Fig. 4 in which $G(s), K(s)$ represent plant and controller and e, y, r, u, d, d_i are the tracking error, output variable, reference input, controlled system input, output disturbance and input disturbance, respectively. Weighting functions of H_∞ design are W_P, W_m, W_u. $\tilde{e}, \tilde{u}, \tilde{y}$ are weighted tracking error, control input and undisturbed system output. The system sensitivity function, $S = (I + GK)^{-1}$, is the transfer function between output y and disturbance d and between tracking error e and the reference input r. Since $\|S\|_\infty$ is a good tool to measure the disturbance rejection and tracking performance of the closed-loop system, a small value of it is appropriate.

In contrast, system complementary sensitivity function, $T = GK(I + GK)^{-1}$, is the transfer function between output y and reference input r. In an ideal situation, $y = r$; so it is desire to have $|T(j\omega)| = 1$ at frequencies of tracking. Since $S + T = I$, to achieve suitable nominal performance and robust stability, it is not possible to make both $\|S\|_\infty$ and $\|T\|_\infty$ small with together. Instead, the weighted sensitivity function, $\|W_P S\|_\infty$, and the weighted complementary sensitivity function, $\|W_m T\|_\infty$, are minimized. W_P is the performance weight which is large enough at low frequencies

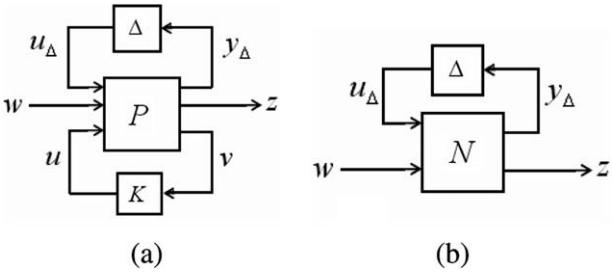

Fig. 3. General control configuration for the case with model uncertainty.

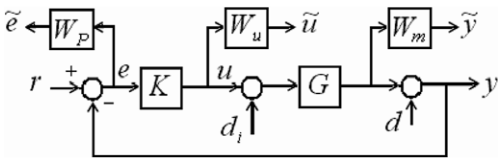

Fig. 4. Schematic of H_∞ design.

where a suitable nominal performance is desired. W_m is an upper bound function on possible multiplicative uncertainties which is large enough at high frequencies where large model uncertainties may occur. Also, to achieve robustness or restrict the magnitude of the input signals, $u = KS(r - d - Gd_i)$, an upper bound $1/|W_u|$ on the magnitude of KS is considered. Usually a stacking approach is used to combine this mixed sensitivity, resulting in the following overall specifications:

$$\|N\|_\infty = \max_\omega \bar{\sigma}(N(j\omega)) < 1; \quad N = \begin{Vmatrix} W_pS \\ W_uKS \\ W_mT \end{Vmatrix}_\infty$$

To measure the size of the matrix N at each frequency, the maximum singular value $\bar{\sigma}(N(j\omega))$ is used. After selecting the form of N and the weights, the H_∞ optimal controller is obtained by solving the problem

$$\min_K \|N(K)\|_\infty$$

where K is a stabilizing controller.

4.2. Obtaining the weight for complex uncertainty

Dynamic uncertainty is not exact and as a result it is difficult to be quantified. However the frequency domain is applied effectively for this class of uncertainty. This results in complex perturbations which are normalized such that $\|\Delta\|_\infty \leqslant 1$. In this paper and many other practical cases, the various sources of dynamic uncertainty can be represented in the form of multiplicative input uncertainty as shown in Fig. 5 and described as

$$G_p(s) = G(s)(1 + W_m(s)\Delta_I(s)); \quad \underbrace{|\Delta_I(j\omega)| \leqslant 1, \quad \forall\omega}_{\|\Delta_I\|_\infty \leqslant 1}$$

where the $G(s)$ and $G_p(s)$ are the nominal and perturbed plants, respectively. $\Delta_I(s)$ is any stable transfer function with a magnitude less or equal to 1, at each frequency. $W_m(s)$ is the weight function and is determined as below:

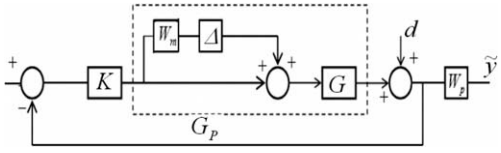

Fig. 5. Feedback system with multiplicative input uncertainty.

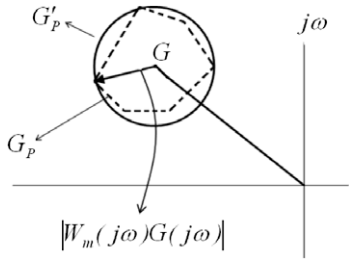

Fig. 6. Disk approximation (solid line) of the original uncertainty region (dashed line).

$$l_I(\omega) = \max_{G_p \in \Pi} \left| \frac{G_p(j\omega)}{G(j\omega)} - 1 \right|, \quad |W_m(j\omega)| \geqslant l_I(\omega), \quad \forall\omega \tag{10}$$

where Π is the set of possible perturbed plant models. In fact, as shown in Nyquist plot in Fig. 6, the original complex uncertainty, $G_p(s)$, is replaced by a conservative disc type approximation, $G'_p(s)$, of radius $|W_m(j\omega)G(j\omega)|$.

4.3. Nominal performance (NP), robust stability (RS) and robust performance (RP)

Consider a SISO system with multiplicative uncertainty as shown in Fig. 5, and assume that the closed loop is nominally stable (NS). The conditions for nominal performance (NP), robust stability (RS) and robust performance (RP) are summarized as [17]

$$NP \iff |W_PS| < 1, \quad \forall\omega \tag{11a}$$
$$RS \iff |W_mT| < 1, \quad \forall\omega \tag{11b}$$
$$RP \iff |W_PS| + |W_mT| < 1, \quad \forall\omega \tag{11c}$$

In general, to analyze NP, RS and RP the structured singular value μ is used (Appendix C). Firstly, the uncertain system is represented in a $N\Delta$ – structure as shown in Fig. 3, where the block diagonal perturbations satisfy $\|\Delta\|_\infty \leqslant 1$. Using Eq. (9) and introducing

$$F = F_u(N, \Delta) = N_{22} + N_{21}\Delta(I - N_{11}\Delta)^{-1}N_{12}$$
$$\text{where} \quad N = \begin{bmatrix} W_mT_I & W_IKS \\ W_PSG & W_PS \end{bmatrix} \tag{12}$$
$$\text{and} \quad T_I = KG(I + KG)^{-1}, \quad S = (I + GK)^{-1}$$

and by considering the robust performance requirement as $\|F\|_\infty \leqslant 1$ for all possible perturbations, yields [17]:

$$NS \iff N \text{ (internally stable)} \tag{13a}$$
$$NP \iff \bar{\sigma}(N_{22}) = \mu_{\Delta_P} < 1, \quad \forall\omega \text{ and } NS \tag{13b}$$
$$RS \iff \mu_\Delta(N_{11}) < 1, \quad \forall\omega \text{ and } NS \tag{13c}$$
$$RP \iff \mu_{\hat{\Delta}}(N) < 1, \quad \forall\omega \text{ and } NS \tag{13d}$$
$$\text{where } \hat{\Delta} = \begin{bmatrix} \Delta & 0 \\ 0 & \Delta_P \end{bmatrix}$$

Δ is a block diagonal matrix that its detailed structure depends on the represented uncertainty and Δ_P is always a full complex matrix indicating the H_∞ performance specification. Δ_P is not necessarily a square matrix.

5. Simulation, discussion and results

In order to simulate the boiler performance, the nominal operating condition of boiler system is considered as [18]:

- Two utility boilers, three CO boilers and two OTSG's are online. The two utility boilers are operated in parallel at equal load.
- Total steam load for 6.306 Mpa collector is 315 kg/s.
- Total electrical output of steam turbine is 145.53 MW.

At this operating point, for each of the two UBs:

$$y_0 = \begin{bmatrix} y_{10} \\ y_{20} \\ y_{30} \end{bmatrix} = \begin{bmatrix} 1.0 \\ 6.47 \\ 466.7 \end{bmatrix}, \quad u_0 = \begin{bmatrix} u_{10} \\ u_{20} \\ u_{30} \end{bmatrix} = \begin{bmatrix} 40.68 \\ 2.102 \\ 0 \end{bmatrix} \tag{14}$$

In addition, the following limit constraints exist for control signals:

$$0 \leqslant u_1 \leqslant 120, \quad 0 \leqslant u_2 \leqslant 7$$

Consider that an increase of 10% in water level of drum y_1, an increase of 5% in drum pressure y_2 and a decrease of 10 percent in the steam temperature y_3 are desired. So with considering Eq. (14), the desired input vector $r(t)$ will be:

$$r(t) = \begin{bmatrix} 1.1\ (\mathrm{m}) \\ 6.77\ (\mathrm{Mpa}) \\ 420\ (^{\circ}\mathrm{C}) \end{bmatrix} \quad (15)$$

Responses of three open-loop systems to the desired input vector $r(t)$ is shown in Fig. 7. As shown, output variables y_1, y_2 and y_3 do not follow the desired inputs of Eq. (15) and the response of system associate with steady state error.

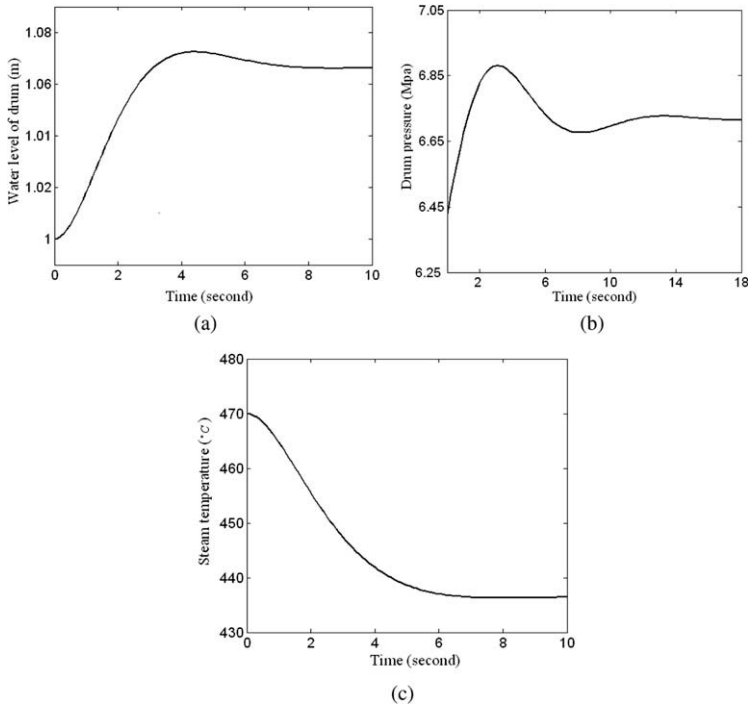

Fig. 7. Time response of open-loop system with respect to (a) 10% increase in water level of drum, (b) 5% increase in drum pressure and (c) 10% decrease in steam temperature.

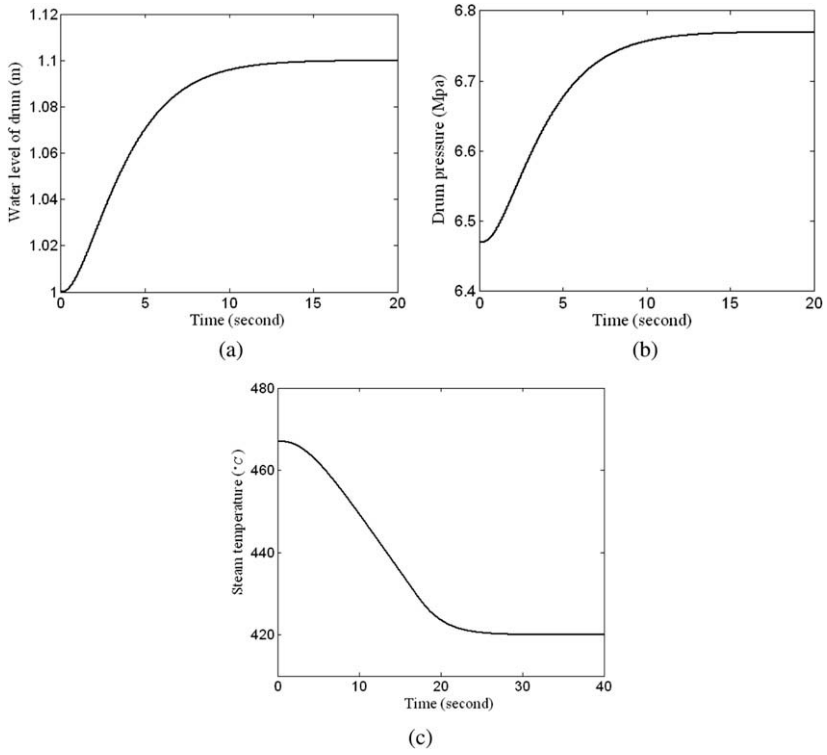

Fig. 8. Time response of the closed-loop system after applying sliding mode controller to (a) 10% increase in water level of drum, (b) 5% increase in drum pressure and (c) 10% decrease in steam temperature.

5.1. Sliding mode controller

A practical example case of boiler performance is considered for simulation with the parameters given in Eq. (2) and Table 1. Consider ±20% uncertainty in these values as

$$\begin{aligned} &0.8\bar{a}_i < a_i < 1.2\bar{a}_i,\\ &0.8\bar{b}_i < b_i < 1.2\bar{b}_i,\\ &0.8\bar{c}_i < c_i < 1.2\bar{c}_i,\\ &0.8\bar{k}_i < k_i < 1.2\bar{k}_i \end{aligned} \tag{16}$$

These ranges of model uncertainties are chosen such that includes the worst case of uncertainties in a practical model of boiler unit. According to Eq. (2), the transfer function between water level of drum y_1 and feedwater mass rate u_1 can be represented as (case-1):

$$y_1^{(3)} = -\bar{a}_1\ddot{y}_1 - \bar{a}_2\dot{y}_1 - \bar{a}_3 y_1 + k_a u_1$$

Comparing the above equation with Eq. (3), yields

$$f = -\bar{a}_1\ddot{y}_1 - \bar{a}_2\dot{y}_1 - \bar{a}_3 y_1$$

Considering the uncertain parameters given in Eq. (16), estimated function $\hat{f}$ can be considered as $\hat{f} = f$. By defining $F = 0.5|f|$, Eq. (5) is satisfied. It is desired to track the desired outputs r_i, so $\ddot{y}_{d_i} = \dot{y}_{d_i} = 0$. According to Eqs. (7) and (8), control law is

$$u_1 = \frac{1.02}{\bar{k}_a} \times \left[\hat{u} - (1.22(F+\eta) + 0.22|\hat{u}|)\cdot sat\left(\frac{s}{\phi}\right)\right]$$

where $s = \ddot{y}_1 + 2\lambda\dot{y}_1 + \lambda^2(y_1 - y_{d_1})$, $\hat{u}$ is constructed according to Eq. (6), and

$$\hat{b}_1 = \left(k_{a_{\min}} \cdot k_{a_{\max}}\right)^{-1/2} = 0.98\bar{k}_a$$
$$\beta_1 = \left(\frac{k_{a_{\max}}}{k_{a_{\min}}}\right)^{1/2} = 1.22\bar{k}_a$$

Also, after several trials to achieve a good performance of controller, the slope of sliding surface, $\lambda = 0.5$; the boundary layer thickness, $\Phi = 0.01$; and $\eta = 10$ are found to be appropriate. Similarly by using the same procedure as mentioned, for case-2 (transfer function between drum pressure y_2 and fuel mass rate u_2) and case-3 (transfer function between steam temperature y_3 and fuel mass rate u_2), the sliding mode controller can be designed.

At the operating point mentioned in Eq. (14) and as shown in Fig. 7, the open-loop system does not track the desired input vector of Eq. (15). Fig. 8 shows the response of the closed-loop system after applying the sliding mode controller in the presence of parametric uncertainties of Eq. (16). As this figure shows, water level of drum y_1, drum pressure y_2 and steam temperature y_3 track the desired inputs $r_1 = 1.1$ m, $r_2 = 6.77$ Mpa and $r_3 = 420\,^{\circ}$C without steady state error. Fig. 9 shows the control signals u_1 and u_2 that satisfy the limit constraints of Eq. (14). Fig. 10 shows the system trajectory for case-1 which starts from $y_1(0) = 1, \dot{y}_1(0) = 0$ and ends to $y_1(0) = 1.1, \dot{y}_1(0) = 0$. Fig. 11 shows the variation of s that satisfies the condition $|s| < \Phi$.

5.2. Robust H_∞ controller

Considering the extreme values of Eq. (16) for perturbed plants G_1, G_2, G_3 and using Eq. (10), the corresponding relative errors $|(G_p - G)/G|$ are found. Fig. 12 shows this error as a-function of frequency for 2^4 resulting G_P's for case-1. According to this figure and similar figures for cases 2 and 3 (that are not shown), the weight functions of model uncertainty are found as

$$\begin{aligned} W_{m1}(s) &= \frac{0.1s + 0.04}{s + 0.03}\\ W_{m2}(s) = W_{m3}(s) &= \frac{0.1s + 0.03}{s + 0.03} \end{aligned} \tag{17}$$

An appropriate performance weight W_P can be represented as [17]:

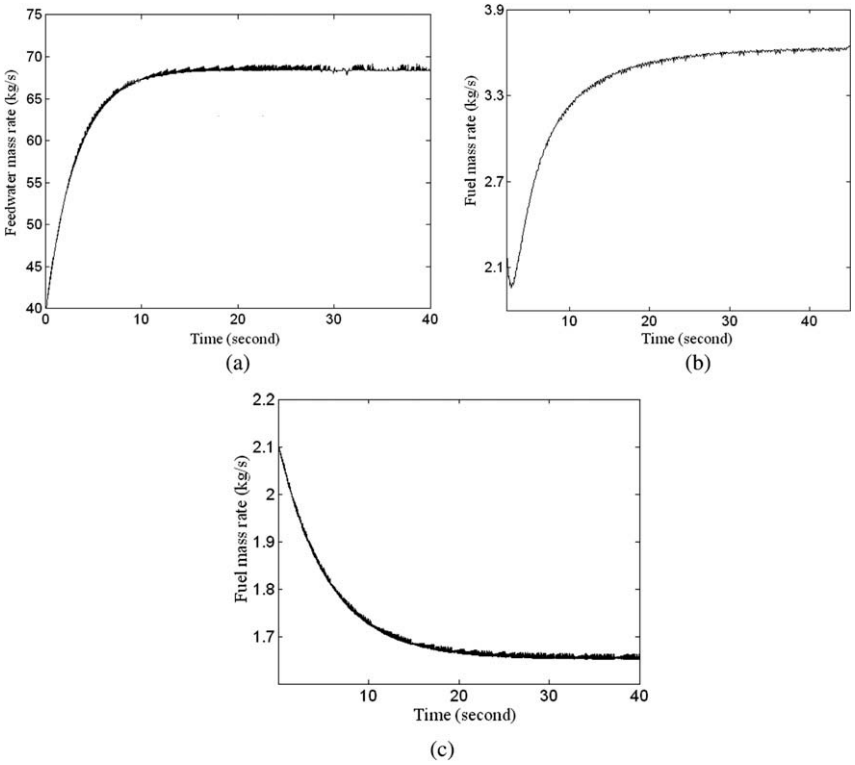

Fig. 9. Variation of control signals of sliding mode controller; feedwater mass rate for (a) 10% increase in water level of drum and fuel mass rate for (b) 5% increase in drum pressure and (c) 10% decrease in steam temperature.

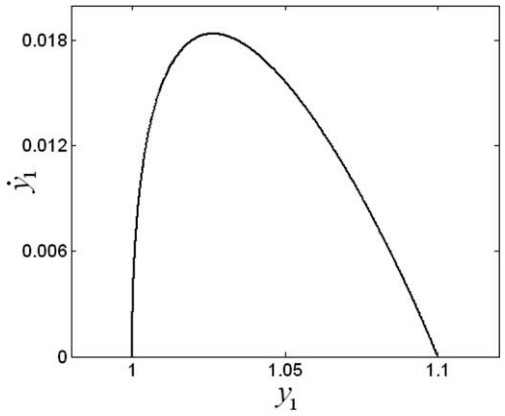

Fig. 10. Sliding surface for the dynamic model.

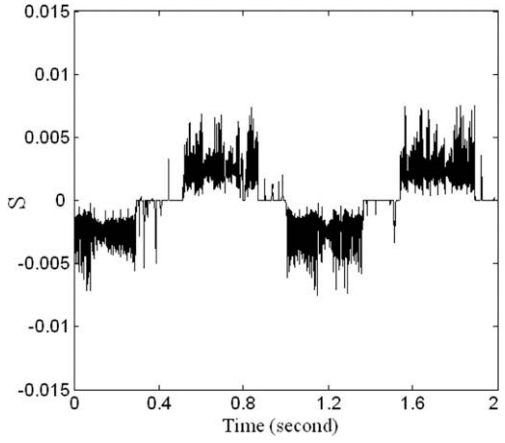

Fig. 11. s-trajectories with time-constant boundary layers.

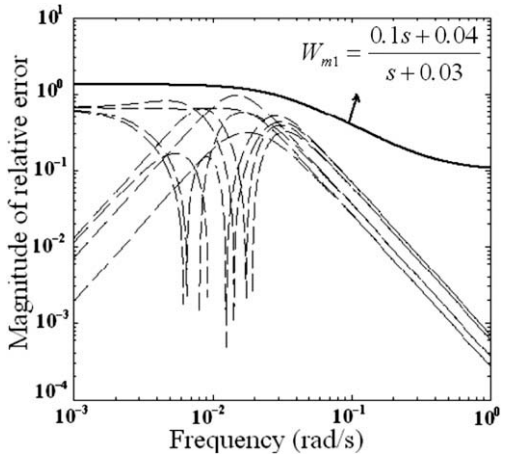

Fig. 12. Relative errors $|(G_p - G)/G|$ for 2^4 perturbed plants of case 1.

$$W_P(s) = \frac{s/M + \omega_B^*}{s + \omega_B^* A}$$

So $1/|W_P|$, the upper bound on $|S|$, is equal to A (typically $A \approx 0$) at low frequencies and is equal to $M \geqslant 1$ at high frequencies, and the asymptote crosses 1 at the frequency ω_B^*, which is approximately the bandwidth requirement. The parameters A, M and ω_B^* are in correlation with steady state tracking error, maximum peak magnitude and speed of time response. To have an appropriate response, a maximum overshoot of 10% and rise time about 2 s, and a perfect tracking (error ≈0), the performance weight is

$$W_P(s) = \frac{s/1.05 + 1.5}{s + 1.5 \times 10^{-4}} \tag{18}$$

Weight functions of Eq. (17), performance weight of Eq. (18) are used in a μ-analysis program using Matlab Robust Control Toolbox. After several trials, the corresponding inverse-based controller which satisfy the robust stability (RS) and nominal performance (NP) are found for three cases as

$$K_{inv,i}(s) = \frac{10}{s^2} G_i^{-1}(s) \quad i = 1, 2, 3$$

$G_i, K_{inv,i}$ and S, SG, KS, T are stable, so the system is nominally stable (NS). Since the sensitivity function $|S|$ and performance weight W_P are the same for all three cases and the uncertainty weights W_m are almost the same, generally the μ-plots for three cases are similar, as shown in Fig. 13. As it is shown, robust stability and nominal performance are satisfied while robust performance is not satisfied in some frequencies (around $\omega = 1$ rad/s). Comparing Eqs. (12) and (13c) show that robust stability (RS) is satisfied if $\|W_m T\|_\infty \leqslant 1$. According to Fig. 13, $\|W_m T\|_\infty = 0.66$, which indicates that the uncertainty may increase by a factor of

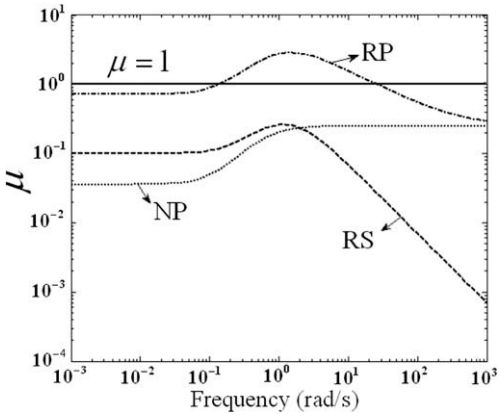

Fig. 13. μ-plots for boiler system with inverse-based controller.

Table 2
Constant values of optimal robust controllers.

λ_1	7.5×10^3	α_1	10	β_1	100
λ_2	2.1×10^2	α_2	5	β_2	40
λ_3	3.2×10^2	α_3	8	β_3	50

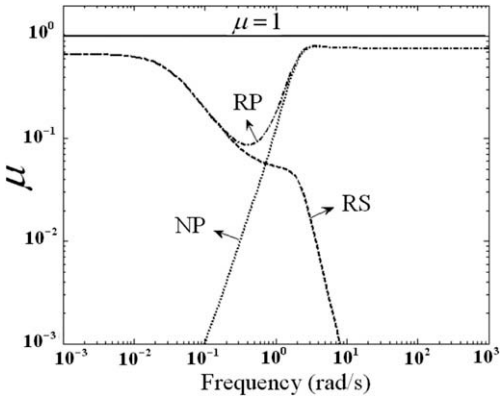

Fig. 14. μ-plots for boiler system after applying optimal robust controller.

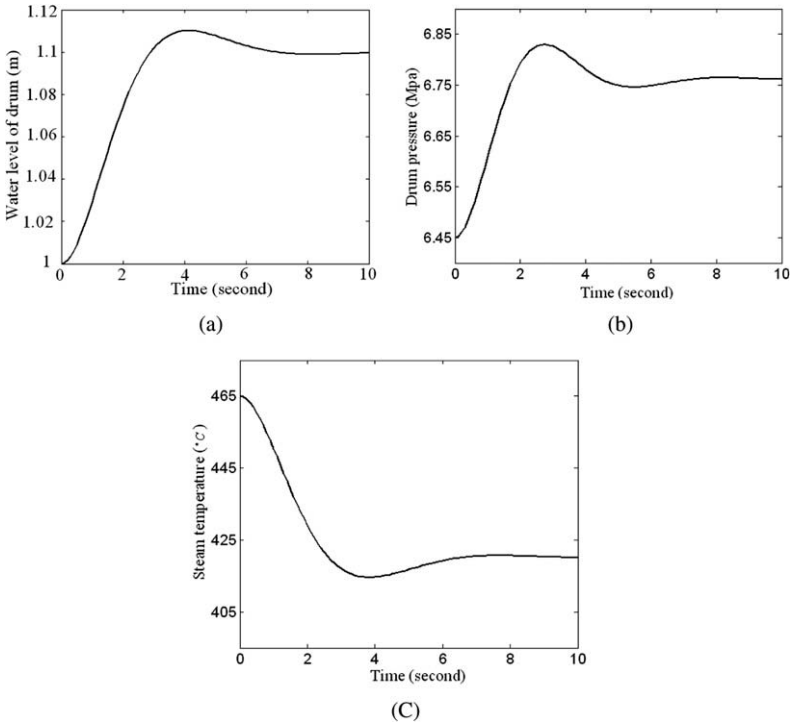

Fig. 15. Time response of the closed-loop system after applying the optimal robust controller to (a) 10% increase in water level of drum, (b) 5% increase in drum pressure and (c) 10% decrease in steam temperature.

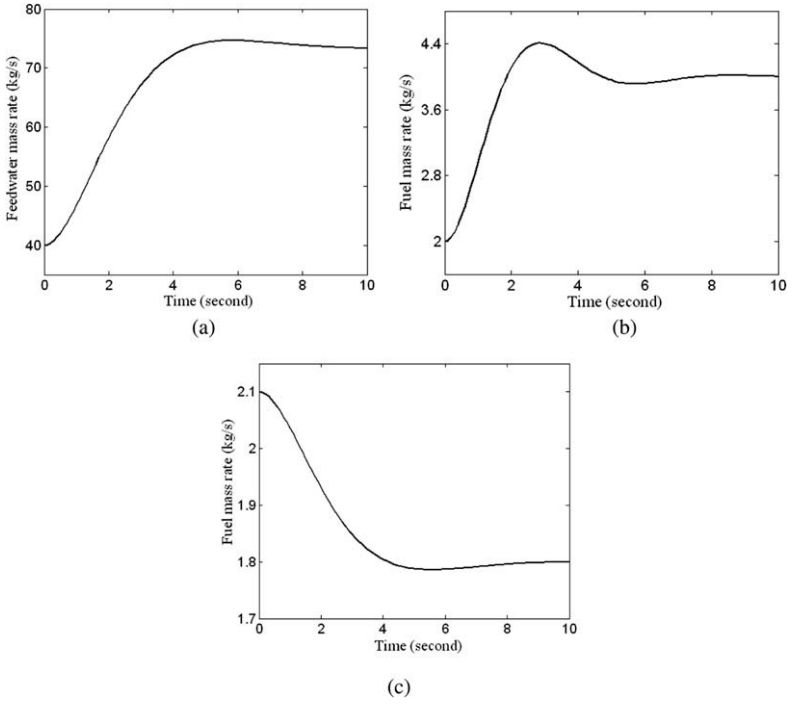

Fig. 16. Variation of control signals of optimal robust controller; feedwater mass rate for (a) 10% increase in water level of drum and fuel mass rate for (b) 5% increase in drum pressure and (c) 10% decrease in steam temperature.

1/0.66=1.51 before the worst-case uncertainty yields instability. Similarly, it can be shown that the $\|KS\|_\infty \leqslant 1$, which indicates that there is no saturation in control signal u.

Since the robust performance is not satisfied, poor time responses of output variables, including water level of drum, drum pressure and steam temperature, are expected. Although an inverse-based controller can be designed easily, it does not exert an appropriate robust performance. To achieve an optimal robust controller a DK-iteration algorithm is applied. However, DK-iteration results in controllers of high orders. For three cases of boiler

model, optimal robust controllers of order 11 are achieved which are approximated with the controllers of order 2, as follows (by using a MATLAB Toolbox and Bode diagram):

$$k_{optimal_i} = \lambda_i \frac{s + \alpha_i}{(s + \beta_i)^2}$$

where the constants $\lambda_i, \alpha_i, \beta_i$ are given in Table 2. Fig. 14 shows the μ-plots for case-1 after applying optimal robust controller 1. μ-plots for cases 2 and 3 can be found in a similar way. According to the Fig. 14, robust stability, nominal performance and robust performance are satisfied.

5.3. A comparison between sliding mode control and robust control

Consider again the Eqs. (14) and (15) which indicate that an increase of 10% in water level of drum y_1, an increase of 5% in drum pressure y_2 and a decrease of 10% in the steam temperature y_3 are desired. As shown in Fig. 7, in open-loop system, output variables do not track the desired inputs without steady state error. Fig. 15 shows the response of the worst perturbed plant after applying the optimal robust controller. In comparison with the results of sliding mode controller as shown in Fig. 8, after applying the optimal robust controller, system track the desired inputs in a less time. For example, the system with optimal robust controller tracks the desired water level of drum (1.1 m) after around 8 s while the system with sliding mode controller tracks it around 18 s. Fig. 16 shows the control signals u_1 and u_2 that satisfy the limit constraints of Eq. (14). In contrary to the Fig. 9 which shows the control signals of sliding mode controller, control signals produced by optimal robust controller are smoother. In addition, in the case of optimal robust control, the control signals reach to their final steady state values in a less time. For example, to track the desire steam temperature (420 °C), fuel mass rate approaches to its final value around 10 s for the optimal robust controller while for the sliding mode controller it is around 28 s. However, the final steady state values of control signals for the optimal robust controller are larger than that of sliding mode. For example, to track the desired drum pressure (6.77 Mpa), the final value of fuel mass rate for optimal robust controller is 4.1 kg/s while for the sliding mode controller is around 3.6 kg/s.

6. Conclusions

In this paper, a linear time invariant (LTI) model of a boiler system is considered in which the input variables are feed-water and fuel mass rates and the output variables are water level of drum, drum pressure and steam temperature. According to the experiment, since the water level of drum is more affected by feedwater mass rate and drum pressure and steam temperature are more affected by fuel mass rate, it is shown that the multi input–multi output dynamic model can be separated to three single input–single output systems. The dynamic model of the boiler may associate with parametric uncertainties. After modelling parametric uncertainties, first a sliding mode controller is designed which guarantees the command tracking objective of the system. Then the parametric uncertainties are represented in the form of multiplicative input uncertainty and μ-synthesis is used to analyze nominal performance, robust stability and robust performance of the uncertain system. Although designing an inverse-base controller is more convenient but it does not guarantee the robust performance of the system. So by using a DK-iteration algorithm, an optimal robust controller is designed which results in robust performance of the system against parametric uncertainties.

In comparison, after applying the optimal robust controller, dynamic system tracks the desired inputs in a less time with respect to the system using sliding mode controller. Also control signals produced by optimal robust controller are smoother and reach to their final steady state values in a less time. However, the final steady state values of control signals (feedwater and fuel mass rates) for the optimal robust controller are larger than that of sliding mode controller which results in more costly efforts.

Appendix A

Consider the Eqs. (14) and (15) which indicate that an increase of 10 percent in water level of drum, an increase of 5% in drum pressure and a decrease of 10% in the steam temperature in Eq. (1) are desired. According to the result of [19], Fig. 17 shows the variation of feedwater mass rate and fuel mass rate as the control signals for an increase of 10% in water level of drum. As Fig. 17 shows, feedwater mass rate must increase from its initial value (40.68 kg/s) to a final value (68 kg/s) while there is no significant change in the fuel mass rate. So it can be concluded that water level of drum is more affected by feedwater mass rate. Fig. 18 shows the variation of feedwater mass rate and fuel mass rate for an increase of 5% in drum pressure [19]. As Fig. 18 shows, fuel mass rate must increase from its initial value (2.1 kg/s) to a final value (3.1 kg/s) while there is no significant change in the feedwater mass rate. So it can be concluded that drum pressure is more affected by fuel mass rate. Similarly it can be shown that steam temperature is more affected by fuel mass rate [19].

Appendix B

Consider a matrix P of dimension $(n_1 + n_2) \times (m_1 + m_2)$ and partition it as [22]

$$P = \begin{bmatrix} P_{11} & P_{12} \\ P_{21} & P_{22} \end{bmatrix} \tag{B.1}$$

Let the matrices Δ and K have dimensions $(m_1 \times n_1)$ and $(m_2 \times n_2)$, respectively (compatible with upper and lower parti-

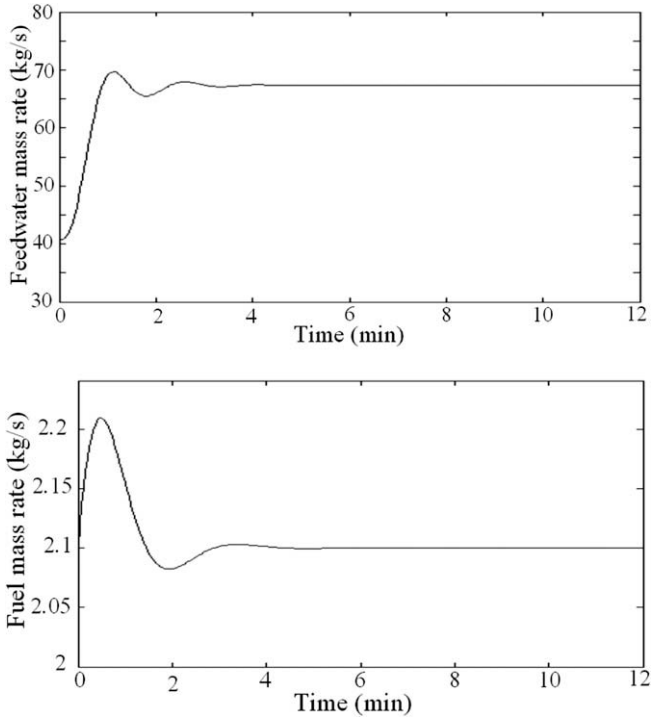

Fig. 17. Variation of feedwater and fuel mass rates, in Eq. (1), for an increase of 10% in water level of drum [19].

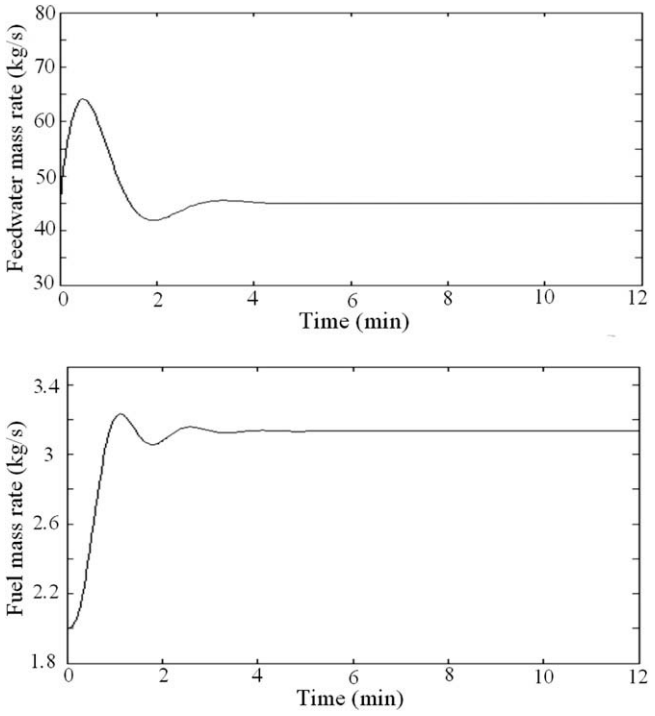

Fig. 18. Variation of feedwater and fuel mass rates, in Eq. (1), for an increase of 5% in drum pressure [19].

tions of P). The following notation for lower and upper linear fractional transformation are defined as

$$F_L(P,K) \triangleq P_{11} + P_{12}K(I - P_{22}K)^{-1}P_{21} \tag{B.2}$$

$$F_u(P,\Delta) \triangleq P_{22} + P_{21}\Delta(I - P_{11}\Delta)^{-1}P_{12} \tag{B.3}$$

Appendix C

Let M be a given complex matrix and let $\Delta = diag\{\Delta_i\}$ denote a set of complex matrices with $\bar{\sigma}(\Delta) \leqslant 1$ and with a given block diagonal structure in which some of blocks may be repeated and some of the blocks may be restricted to be real. Real non-negative function $\mu(\Delta)$ called the structural singular value, is defined by [22]

$$\mu(M) = \frac{1}{\min\{k_m | \det(I - k_m\Delta M) = 0 \text{ for structure } \Delta; \quad \bar{\sigma}(\Delta) \leqslant 1\}}$$

If no such structured Δ exists then $\mu(M) = 0$. A value of $\mu = 1$ means that there exists a perturbation with $\bar{\sigma}(\Delta) = 1$ which is just large enough to make $I - M\Delta$ singular. A large value of μ is bad as it means that a smaller perturbation makes $I - M\Delta$ singular, whereas a smaller value of μ is good.

References

[1] Chen PC, Shamma JS. Gain-scheduled l^1-optimal control for boiler–turbine dynamics with actuator saturation. Int J Process Control 2004;14:263–77.
[2] Moradi H, Alasty A, Bakhtiari-Nejad F. Control of a nonlinear boiler–turbine unit using two methods: gain scheduling & feedback linearization. In: ASME international mechanical engineering congress & exposition, IMECE2007-43945; 2007.
[3] Tan W, Marquez HJ, Tongwen C, Liu J. Analysis and control of a nonlinear boiler–turbine unit. Int J Process Control 2005;15:883–91.
[4] Bell RD, Astrom KJ. Dynamic models for boiler–turbine-alternator units: data logs and parameter estimation for a 160 MW unit. Technical report LUTFD2/(TFRT-3192)/1-137. Lund, Sweden: Department of Automatic Control, Lund Institute of Technology; 1987.
[5] Rusinowski H, Stanek W. Neural modelling of steam boilers. J Energy Convers Manage 2007;48:2802–9.
[6] Kim H, Choi S. A model on water level dynamics in natural circulation drum-type boilers. J Int Commun Heat Mass Transfer 2005;32:786–96.
[7] Rink R, White D, Chiu A, Leung R. SYNSIM: a computer simulation model for the Mildred Lake steam/electrical system of Syncrude Canada Ltd., University of Alberta, Edmonton, AB, Canada; 1996.
[8] Kocaarslan I, Cam E. An adaptive control application in a large thermal combined power plant. J Energy Convers Manage 2007;48:174–83.
[9] Abdennour A. An intelligent supervisory system for drum type boilers during severe disturbances. J Electr Power Energy Syst 2000;22:381–7.
[10] Prasad G, Swidenbank E, Hogg BW. A local model networks based multivariable long-range predictive control strategy for thermal power plants. J Automat 1998;34(10):1185–204.
[11] Dimeo R, Lee KY. Boiler–turbine control system design using a genetic algorithm. IEEE Trans Energy Convers 1995;10(4):752–9.
[12] Alturki FA, Abdennour AB. Neuro-fuzzy control of a steam boiler–turbine unit. In: Proceedings of IEEE international conference on control applications, Hawaii; 1999. p. 1050–5.
[13] Liu XJ, Lara-Rosano F, Chan CW. Neurofuzzy network modelling and control of steam pressure in 300 *MW* steam-boiler system. J Eng Applicat Artif Intell 2003;16:431–40.
[14] Kwon WH, Kim SW, Park PG. On the multivariable control of robust control of a boiler–turbine system. In: IFAC symposium on power systems & power plant control, Seoul, Korea; 1989. p. 219–23.
[15] Pellegrinetti G, Bentsman J. H_∞ controller design for boilers. Int J Robust Nonlinear Control 1994;4:645–71.
[16] Tan W, Niu YG, Liu JZ. H_∞ control for a boiler–turbine unit. In: Proceedings of IEEE conference on control applications, Hawaii, USA; 1999. p. 807–10.
[17] Skogestad S, Postlethwaite I. Multivariable feedback control. New York: John Wiley and Sons; 2005.
[18] Tan W, Marquez HJ, Chen T. Multivariable robust controller design for a boiler system. IEEE Trans Control Syst Technol 2002;10(5):735–42.
[19] Moradi H, Alasty A, Thaghavi S. Applying eigenstructure assignment to design regulator and tracking systems for a boiler unit. In: 16th annual (international) conference on mechanical engineering, ISME2008-1863, May 14–16, Kerman, Iran; 2008.
[20] Nanhua Y, Wentong M, Ming S. Application of adaptive Gray predictor based algorithm to boiler drum level control. J Energy Convers Manage 2006;47:2999–3007.
[21] Slotine JJ, Li W. Applied nonlinear control. Englewood cliffs, NJ: Prentice Hall Inc.; 1991.
[22] Doyle JC. Lecture notes on advances in multivariable control. ONR/Honeywell workshop, Minneapolis, USA; 1984.